

Pt black catalyzed methane oxidation to methyl bisulfate in H₂SO₄-SO₃Hee Won Lee^{a,b,1}, Huyen Tran Dang^{a,b,1}, Honggon Kim^a, Ung Lee^a, Jeong-Myeong Ha^{a,b},
Jungho Jae^c, Minserk Cheong^d, Hyunjoon Lee^{a,b,*}^a Clean Energy Research Center, Korea Institute of Science and Technology, 5 Hawrang-ro 14-gil, Sungbuk-gu, Seoul 02792, Republic of Korea^b Division of Energy & Environment Technology, KIST School, Korea University of Science and Technology, Seoul 02792, Republic of Korea^c School of Chemical and Biomolecular Engineering, Pusan National University, Busan 46241, Republic of Korea^d Department of Chemistry and Research Institute of Basic Sciences, Kyung Hee University, 26 Kyunghedae-ro, Dondaemun-gu, Seoul 02447, Republic of Korea

ARTICLE INFO

Article history:

Received 21 February 2019

Revised 19 April 2019

Accepted 24 April 2019

Keywords:

Methane

Oxidation

Pt black

Oleum

Methyl bisulfate

ABSTRACT

Although chloride-ligated Pt compounds like (bpym)PtCl₂, K₂PtCl₄, and (DMSO)₂PtCl₂ has been reported to be highly active catalysts for the methane oxidation to methyl bisulfate (MBS) in oleum media, their applications is hampered by the catalyst deactivation to PtCl₂. In this study, we investigated Pt black catalyzed methane oxidation, which has no ligand. A MBS yield of 82.1% with a selectivity of 96.5% was obtained at a catalyst loading of 1.6 mM at 180 °C, which proved the highest catalytic activity of Pt-black for this reaction. The reaction was thought to proceed by the dissolved Pt species, and no deactivation was observed during four consecutive experiments. However, at a concentration of over 30 mM, MBS yield fell due to the decomposition of MBS to CO₂ on the surface of heterogeneous Pt(0). Vacuum distillation experiments showed the potential for isolating MBS from the oxidation product mixture as a major component.

© 2019 Elsevier Inc. All rights reserved.

1. Introduction

Methane is one of the most abundant and inexpensive hydrocarbon resources on the earth. However, due to its thermochemical stability, its direct conversion to value-added materials like methanol is still challenging [1–4]. Currently, the conversion of methane to methanol is carried out using an energy-consuming two-steps process; reforming methane to a syngas (a mixture of CO and H₂) at a temperature above 800 °C, and conversion of the syngas to methanol using heterogeneous catalyst system at the temperature of 150–300 °C.

Over the decades, the direct oxidation of methane to methanol has been studied extensively, however, because methanol is more reactive than methane in the oxidation condition, methanol cannot be obtained at high yield [5–8]. One way of achieving high product yield in methane oxidation is to convert methane to methanol precursors like methyl bisulfate (CH₃OSO₃H, MBS) or methyl trifluoroacetate (CF₃CO₂CH₃) by conducting the reaction in oleum (SO₃-H₂SO₄) [9–11] or trifluoroacetic acid, respectively [2,12–18]. In particular, oxidation to MBS is reported highly likely to be commercialized because the oxidant used, SO₃, is air-regenerable and

inexpensive. Furthermore, highly active catalysts such as iodine compounds [19–22] and Pt complexes [23,24] are also being developed.

The use of oleum for the oxidation of methane was first reported by R. A. Perana et al., who demonstrated the synthesis of MBS using a Hg(SO₄)₂ catalyst [24]. In 1998, the same research group announced a very stable Pt catalyst, (bpym)PtCl₂ which was known to have a TON of 500 and MBS yield of over 70% [9]. Since then, various Pt systems like PtCl₂-ionic liquids [25], Pt on CTF [26] or Pt on polybenzimidazole [27] have been published as a catalysts for the methane oxidation in an oleum system. Some kinds of iodine material have been reported to activate methane to MBS and the active catalytic species was estimated to be I₂HS₂O₇⁻ [25].

T. Zimmerman et al disclosed a new findings that various Pt compounds, including PtCl₂, K₂PtCl₄ and Pt(acac)₂, could catalyze methane oxidation to MBS [11,23]. The TOF reached over 20000, which could move the reaction one step closer to the commercialization. By conducting the reactions for short times, less than 5 min, they could examine the intrinsic catalytic activity of various Pt catalyst.

Recently, we found that DMSO-bonded PtCl₂, (DMSO)₂PtCl₂, has an enhanced methane oxidation activity by stabilizing Pt species in oleum [25]. It showed increased stability at the reaction conditions compared to K₂PtCl₄ and increased catalytic activity compared to

* Corresponding author.

E-mail address: hjlee@kist.re.kr (H. Lee).¹ These authors contributed equally to this work.

(bpym)₂PtCl₂. In the (DMSO)₂PtCl₂ system, MBS yield and selectivity reached 84% and 94%, respectively, at a catalyst concentration of 3.0 mM at 180 °C for 3 h reaction and it achieved over 19,000 turnovers at a low catalyst concentration. However, although it could be reactivated to some extent by adding DMSO, (DMSO)₂-PtCl₂ was deactivated to PtCl₂ after the reaction like the other Pt compounds with chloride ligand.

This result motivated us to investigate another Pt catalyst that has no ligand, Pt black. In fact, the intrinsic catalytic activity of Pt black for methane oxidation had already been reported by T. Zimmerman et al along with other Pt compounds. They determined Pt black had TOF of 20200/h and TOs of 840 during 2.5 min at 215 °C.

Based on this previous report, we conducted Pt black-catalyzed methane oxidation in oleum-media to understand the optimum conditions for MBS yield and catalyst reusability. The reaction mechanism for Pt black-catalyzed methane oxidation was also estimated using a DFT calculation. Finally, vacuum distillation was conducted to isolate the MBS from the product mixture.

2. Experimental

2.1. Chemicals

All chemicals were of analytical reagent grade and used without further purification. Oleum (20 wt%, and 65 wt%) were obtained from Aldirch Chemical. Pt-black of 27 m²/g was purchased from Alfa Aesar. CH₄ (99%) containing 1% of Ar was supplied by Shinyang Gas Co.

2.2. Oxidation reaction

Methane oxidation using Pt black was conducted as same method described in our previous paper using stainless steel reactor (SS 316) equipped with glass liner, thermocouple, and heating jacket [25]. The reactor containing catalyst and 30 g of 20%wt oleum (SO₃, 75 mmol) was pressurized with 25 bar of CH₄ at room temperature. With stirring the solution using Teflon-coated magnetic bar with 800 rpm, reactor was heated to 180 °C. During the reaction, the pressure was maintained to 35 bar. After the reaction, the reactor was cooled to room temperature and the remaining gas was vented in the hood.

2.3. Analysis

Liquid product containing methyl bisulfate was analyzed using ¹H NMR (400 MHz, Varian). Calibration curve was made using sodium bisulfate (CH₃OSO₃Na) and methane sulfonic acid (CH₃SO₃-H) as an external standard in D₂SO₄. In order to evaluate the CO₂ formation, the gas phase product was captured, washed with distilled water, and analyzed using GC-MS (HP 6890 GC with a 5973 Mass spectrometer selective detector) equipped with capillary column (Poraplot Q 30 m × 25 μm). The peak areas of Ar which was included in methane (1%) was used as a reference to determine the concentration of CO₂. The Platinum concentration in the liquid phase was also examined by ICP-OES technique (Thermo scientific iCAP 700 series-ICP spectrometer). The X-ray diffraction patterns (XRD) were recorded on a Shimadzu X-ray diffractometer (XRD-6000, Japan) using nickel-filtered CuKα radiation with 2θ angle from 10 to 80°. Raman spectra were measured using a TruScan GP (ThermoScientific, 785 nm). Quantitative energy-dispersive X-ray spectroscopy (EDS) analysis was conducted on a field emission electron microscope (FEI Teneo VS) at an acceleration voltage of 20 kV.

Yield of MBS and selectivities of MBS and CO₂ were calculated according to the reaction equation in Scheme 1. Because the reaction was conducted at a constant pressure of 35 bar, the yield of MBS was decided based on the amount of SO₃ used instead of methane consumption. Conversion of CH₄ and SO₃ were calculated based on the synthesized amount of MBS and CO₂.

$$\text{Yield (MBS, \%)} = 100 \times \frac{\text{MBS produced (mmol)}}{\text{SO}_3 \text{ used (mmol)}/2}$$

$$\text{Selectivity (MBS or CO}_2\text{, \%)} = 100 \times \frac{\text{MBS or CO}_2\text{, produced (mmol)}}{\text{MBS produced (mmol)} + \text{CO}_2 \text{ produced (mmol)}}$$

$$\text{Conversion (CH}_4\text{, \%)} = 100 \times \frac{\text{MBS} + \text{CO}_2\text{, produced (mmol)}}{\text{SO}_3 \text{ used (mmol)}/2}$$

$$\text{Conversion(SO}_3\text{, \%)} = 100 \times \frac{\text{MBS} \times 2 + \text{CO}_2 \times 6, \text{ produced (mmol)}}{\text{SO}_3 \text{ used (mmol)}}$$

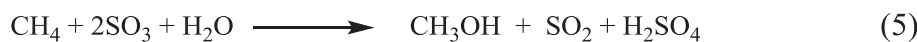
Step 1. Oxidation



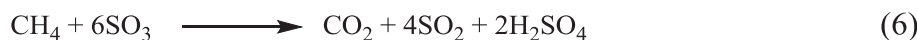
Step 2. Hydrolysis



Net Reaction



CO₂ Formation



Scheme 1. Reaction steps of methane oxidation to methanol via methyl bisulfate (CH₃OSO₃H, MBS) in H₂SO₄-SO₃ system.

2.4. Vacuum distillation

The oxidation product containing MBS was transferred to the apparatus shown in Fig. S1 in the Supporting information, and vacuum distillation was conducted as described in the Supporting information. Distillation proceeded until no more product was collected in the receiver. After the distillation, distillation residue and distilled product were analyzed using ^1H NMR and Raman spectroscopy to calculate the amount of MBS in the solution and to estimate the purity of the product, respectively.

2.5. Computational detail

All calculations were carried out using Gaussian 16 (Revision A.03. Gaussian, Inc., Wallingford CT). All ground-state and transition-state geometries were optimized at the B3LYP level of theory. Basis sets selected for these calculations are the 6-31G(d, p) for C, H, N, O, S, and Cl and LANL2DZ for Pt. Geometries were confirmed as minima or transition-state structures by normal-mode vibrational frequency analysis. Exhaustive conformational searching was performed for all ground-state and transition state structures, but only the lowest-energy structures are reported. Calculations were performed for reactions in the liquid phase, so the SMD polarizable continuum solvent model augmented with parameters for sulfuric acid (static ($\epsilon_{\text{ps}} = 101$) and optical ($\epsilon_{\text{psinf}} = 2.042$) dielectric constants) was used.

3. Results and discussion

Methane oxidation to methanol via methyl bisulfate (MBS) in oleum ($\text{H}_2\text{SO}_4\text{-SO}_3$) is comprised of two reactions, oxidation and hydrolysis, as shown in Eqs. (1)–(4) in Scheme 1. First, methane oxidizes to MBS in oleum with the formation of SO_2 and water. Because the water reacts with SO_3 to form H_2SO_4 , methane consumes 2 equiv. of SO_3 at the oxidation. MBS hydrolyzes to methanol and sulfuric acid as in Eq. (4). Accordingly, the net reaction from methane to methanol can be expressed as Eq. (5) in Scheme 1; one mole of methane reacts with two moles of SO_3 and one mole of water to make one moles of methanol, SO_2 and sulfuric acid. In the case of CO_2 , 6 equiv. of SO_3 is consumed from methane to CO_2 .

3.1. Effect of catalyst concentration

T. Zimmerman et al investigated the effect of catalyst concentration on the absolute rate of MBS formation (γ_{MBS}) and reported that K_2PtCl_4 had the highest γ_{MBS} for the methane oxidation at 0.6 mM catalyst concentration. Similarly, we also found that K_2PtCl_4 had the highest MBS yield of 62% at a catalyst concentration of 0.77 mM and the yield decreased to 40–50% at the catalyst concentration higher than that. In both reports, the concentration effect was attributed to the formation of less active PtCl_2 from K_2PtCl_4 , and the co-released chloride anion aggravated the catalytic activity of PtCl_2 even more.

For this Pt black-catalyzed reaction, we found the yield of MBS also reached a maximum value at 1.6 mM catalyst concentration, but the reason for the decreased yield at a higher catalyst concentration was found not to be caused by catalyst deactivation, but because of the over-oxidation of MBS to CO_2 .

Methane oxidation using Pt black in the presence of oleum (20% wt SO_3) was conducted at 180 °C for 3 h under 35 bar of methane pressure. In Table S2 and Fig. 1, the effect of catalyst amount on the yield of MBS and selectivities to MBS and CO_2 were marked together with the conversion of methane and SO_3 , which were determined as described in the experimental section.

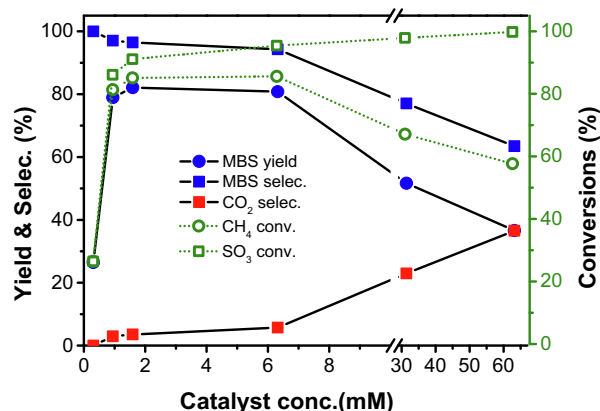


Fig. 1. Effect of Pt-black concentrations on the Pt-black catalyzed methane oxidation to methyl bisulfate (MBS). Conditions: oleum (20%wt SO_3), 35 bar of CH_4 , 180 °C, 3 h.

As can be seen in Fig. 1, the yield of MBS at a low catalyst concentration of 0.31 mM was 26.4%. When the catalyst concentration increased, the MBS yield reached maximum at 1.6 mM with a yield of 82.0%, which is a very similar value obtained at (DMSO) $_2\text{PtCl}_2$ -catalyzed reaction [25]. At catalyst concentrations between 0.94 and 6.30 the change in MBS yield was marginal. However, when the Pt black concentration increased to 31.5 mM, the formation of MBS decreased to 51.7% and further decreased to 36.5% at 63.2 mM Pt black concentration. The analysis of CO_2 concentration after the reaction revealed the decrease in MBS formation could be attributed to the formation of CO_2 . At a catalyst concentration less than 2 mM, the formation of CO_2 was not significant, but its formation increased substantially at the higher catalyst concentrations. When the selectivity to CO_2 was calculated with respect to the amount of MBS, it reached to 22.9% and 36.6% at 31.5 mM and 63.2 mM catalyst concentration, respectively.

The advantage of this oleum mediated methane oxidation is the high conversion of methane and high selectivity to a methanol intermediate, MBS, due to the stability of MBS in this oxidation condition [2,10]. However, this benefit was lost at high concentration of Pt black catalyst. Fig. 2 and Table S3 show, at 1.6 mM, the MBS yields for 1 h and 3 h were 57.3% and 82.1%, respectively. After 12 h, the MBS yield was 82.4%. However, at 63.2 mM, the MBS yield of 54.9% after 1 h oxidation fell to 36.5% after 3 h reaction and decreased to 10.1% after 12 h with an increase in CO_2 formation. These results indicate that MBS is very stable at 1.6 mM

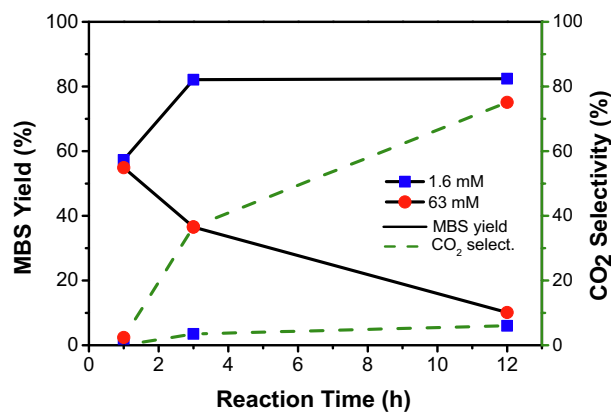


Fig. 2. Effects of reaction time on the MBS yield and CO_2 selectivity at the Pt black catalyzed reaction of different Pt concentration. Conditions: oleum (20%wt) 30 g, 35 bar of CH_4 , 180 °C.

catalyst concentration, but it is oxidized to CO_2 at a higher concentration of Pt black catalyst. We assume the low stability of MBS at higher Pt concentration may be due to the heterogeneous Pt in the reaction solution.

When 20 mg of Pt black was used for the reaction in 30 g oleum condition, ~ 16 mg of solid Pt could be isolated after the reaction. ICP analysis of the Pt concentration after the reaction revealed Pt ions in the product solution were 2.7 mg in 30 g product solution, which corresponds to 0.85 mM. Moreover, the experimental finding that the highest MBS yield could be obtained at a catalyst concentration at 1.6 mM (5.0 mg in 30 g solution) supports the conclusion that Pt black dissolution in oleum (20 wt%) might be between 0.85 and 1.6 mM. Accordingly, the high CO_2 formation at the reaction conducted using large amounts of catalyst indicates that the decomposition of MBS to CO_2 can happen on the surface of heterogeneous Pt(0), not by dissolved Pt ion.

On the surface of Pt black, besides the oxidation of MBS to CO_2 , coke formation was observed. SEM, XPS and XRD analyses of the isolated Pt black showed its morphology and oxidation state were almost similar to those of fresh Pt-black (Fig. 3 and Fig. S2–S4). However, interestingly, SEM-EDX analyses revealed the surface carbon amount was increased from 4.5% to 16.2% (Table 1 and Table S4). Furthermore, BET analyses showed the surface area of Pt black had decreased from 29.4 to 8.1 m^2/g after the reaction, presumably due to the carbon deposition on the surface. The XPS analyses shown in Fig. S4 reveal the form of the deposited carbon on the Pt surface was almost identical to the fresh Pt black, indicating the carbon on the surface of Pt was in an amorphous form. On the other hand, sulfur deposition was insignificant after the reaction.

3.2. Reuse of catalyst

Although the origin and formation mechanism of carbon on the surface of Pt black were not investigated in detail, it was found to affect catalytic activity when the catalyst was reused. When the heterogeneous Pt black isolated after the reaction was reused, the yield of MBS was gradually decreased with the reuse (Fig. 4). Analyses of the dissolved Pt concentration in the product mixture after each reuse revealed the concentration of homogeneous Pt decreased with the reuse, presumably due to the prevention of Pt dissolution by the surface carbon. However, this limitation might be overcome by air-oxidation of the used Pt black at a temperature that wouldn't affect to the surface area of the Pt black.

More important issue is understanding the deactivation of the dissolved Pt in the product solution. As we mentioned in the introduction, chloride-ligated Pt compounds deactivated to PtCl_2 during the reaction. However, in this Pt black-catalyzed reaction, because

there is no chloride in the reaction system, there is no reason for catalyst deactivation associated with the formation of PtCl_2 on the dissolved Pt species. To verify this issue, we conducted 2 kinds of reaction sets which were composed of 4 consecutive methane oxidation reactions. In Rxn 1, Pt black (20 mg) was added at the first reaction and no catalyst was added after that, while in Rxn 2, 5 mg of Pt black was used at the first reaction and 5 mg fresh catalyst was added before each new reaction. In both reaction, new oleum (65%, 75 mmol of SO_3) was added after the each methane oxidation. Table 2 shows, as the reaction rounds increased, the yields of MBS decreased with a substantial degree for both reactions. This is not because of the change of the Pt concentration between 1.6–6.3 mM. In this concentration range, the MBS yield was very similar as can be seen from Fig. 1. Rather, this may be due to the increase of total volume of the solution, which could affect to contact area of gaseous methane with the solution, dissolution speed in sulfuric acid solution and SO_3 concentration. However, similar MBS yields were observed in Rxn 1 and Rxn 2, indicating the deactivation of dissolved Pt species was negligible for this Pt black catalyzed reaction.

Table 1

Comparison of carbon content and surface area of Pt-black before and after the reaction.

Analysis	Before	After
Carbon content (wt%, SEM-EDX)	4.5	16.2
BET surface area (m^2/g)	29.4	8.1

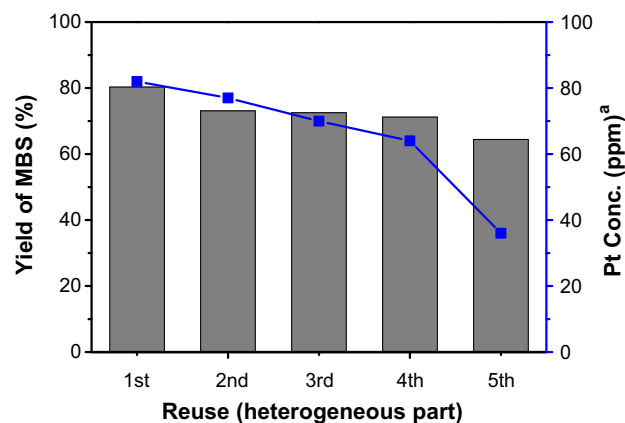


Fig. 4. Reuse of heterogeneous Pt black in the methane oxidation. Conditions: oleum (20%wt SO_3) 30 g, Pt black 20 mg, CH_4 35 bar, 180 °C, 3 h. ^a Pt concentration dissolved in product solution (mg Pt/kg solution).

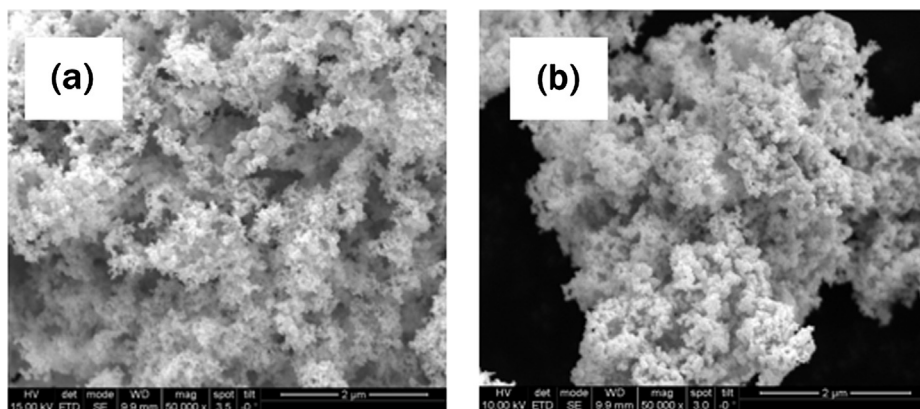


Fig. 3. SEM images of Pt-black (a) before and (b) after the reaction.

Table 2
Consecutive methane oxidation reaction using Pt-black catalyst.

Reaction round	Rxn 1 ^a		Rxn 2 ^b	
	MBS Yields (%) ^c	Pt Con. (mM)	MBS Yields (%) ^c	Pt Con. (mM)
1st	82.1	6.3	82.5	1.6
2nd	78.7	4.8	70.5	2.4
3rd	50.8	3.9	49.2	2.9
4th	46.7	3.3	44.2	3.3

^a Reaction condition: 30 g of 20 wt% oleum, Pt black 20 mg, 180 °C, 35 bar CH₄, 3 h. After each reaction, 9.23 g of 65 wt% oleum was added for next reaction.
^b Reaction was conducted with a same way as Rxn 1 except 5 mg of Pt black was used at 1st reaction. After each reaction, fresh 5 mg of Pt black and 9.23 g of 65 wt% oleum was added for next reaction.
^c Yield of MBS for each reaction round was determined by subtracting the amount of MBS synthesized at the previous reaction round from the total amount of MBS analyzed.

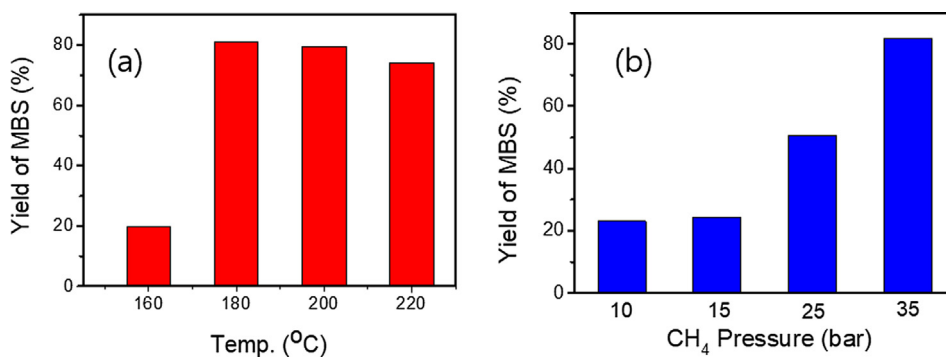


Fig. 5. Effects of (a) reaction temperature and (b) CH₄ pressure on the Pt black catalyzed methane oxidation reaction. Condition: oleum (20%wt) 30 g, Pt black 1.6 mM, 3 h.

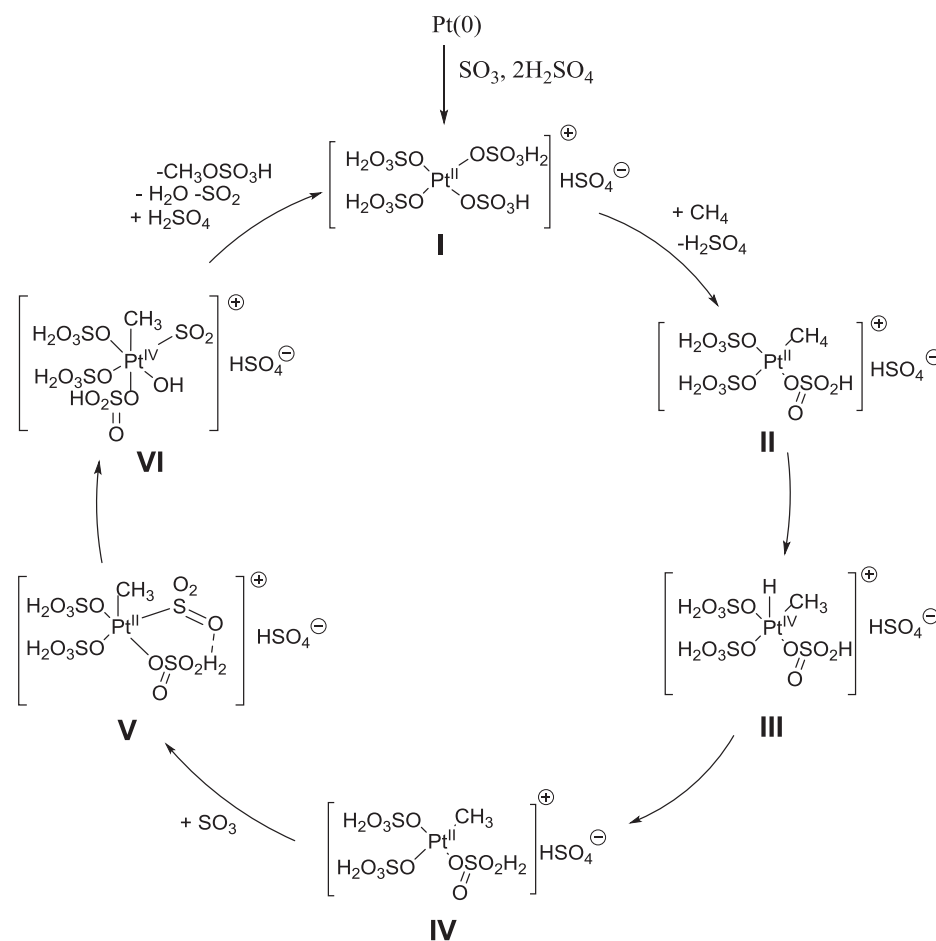


Fig. 6. Proposed mechanism of Pt-black catalyzed methane oxidation to methylbisulfate (MBS).

3.3. Effects of reaction condition

The effects of reaction temperature and reaction time on this Pt black-catalyzed reaction were investigated and the results are depicted in Fig. 5(a) and (b). At 160 °C, the yield of MBS was 19.6%. By increasing the reaction temperature to 180 °C, the yield of MBS sharply increased to 82.0%, and then slightly decreased at the temperature of 200 and 220 °C, presumably due to the decomposition of MBS to CO₂. The methane pressure also had a significant effect on the MBS yield because methane can be dissolved in a reaction mixture at a higher pressure. At 10 and 15 bar, the yield of MBS was 23.1 and 24.4%. When the pressure increased to 25 and 35 bar, the yields of MBS increased to 50.5% and 82.1%.

3.4. Reaction mechanism

Based on the above discussion, it seems that Pt black dissolved in oleum was oxidized to Pt(II) to form a cationic sulfuric acid-coordinated Pt(II) species, Pt(II)(OSO₃H)(H₂SO₄)⁺ as depicted Fig. 6. Then, sulfuric acid dissociated from the Pt center to create a vacant site for methane coordination. C-H bond activation of the methane happened by the oxidative addition to Pt, making the species III. Reductive elimination of the sulfuric acid formed a species IV, and the successive addition of SO₃ resulted in species V. The SO₃ in species V can be protonated by the nearby H₂SO₄ ligand, and oxidative addition can happen to form SO₂ and the OH coordinated Pt species, VI. Reductive elimination of the MBS and ligand dissociation of H₂O, SO₂, and sulfuric acid association form the starting species I. The energy diagram based on the DFT calculation is shown in Fig. S5.

3.5. Distillation

Although high performance methane oxidation catalysts such as Pt compounds and iodine material with activities high enough to be commercialized have been developed, many challenges still exist for the practical application of this oleum-mediated methane oxidation. One of the issues is related to MBS separation from the reaction product mixture. However, as far as we know, there has been no report about the isolating of MBS from a sulfuric acid media except in the patent literatures [28–30]. According to the patents, dimethyl sulfate (DMS) was isolated during the vacuum distillation of MBS-H₂SO₄ solution, suggesting the possibility of disproportionation of MBS to DMS. However, we obtained a different result; MBS was obtained as a major product.

In this study, distillation was conducted as described in the experimental section and supporting information. When 102.60 g of product solution containing 10.10 g (92.3 mmol) of MBS was distilled under a vacuum condition of 0.1 mbar at 130–145 °C during 3 h, 9.63 g of liquid was collected in the receiver 1 (R1). NMR analysis of the distillate product revealed the MBS amount in R1 was 8.58 g (76.6 mmol), which corresponds to 82.9% of the MBS amount in the oxidation product. The other 1.05 g in the R1 was assumed to be the mixture of H₂SO₄ and SO₃. On the other hand, besides the distillation product in R1, about 1.13 g of white solid was collected in receiver 2 (R2) immersed in the liquid nitrogen, which is thought to be the SO₃/SO₂ mixture. The mass balance of the distillation in Table S1 reveals there was some loss during distillation, indicating some SO₃ or SO₂ was transferred to the vacuum pump.

Although ¹H NMR analysis of the distilled product showed one single peak, Raman analyses revealed DMS was also contained in the distilled product. In ¹H NMR, MBS and DMS appeared at the same position (Fig. S6 in supporting information), but Raman spectra clearly distinguish MBS and DMS although the quantitative analysis is not feasible. Fig. 7 shows SO₂ rocking vibration in

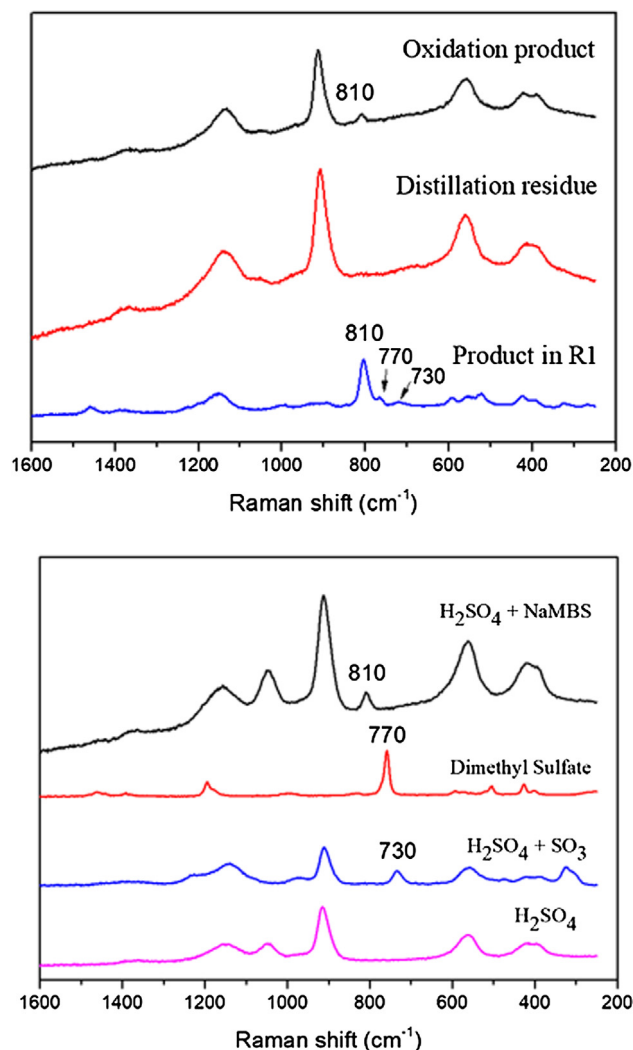


Fig. 7. Raman Spectra of the reagents and vacuum distillation product.

SO₃-H₂SO₄ appears at 730 cm⁻¹ [31]. While, those of DMS and MBS appeared at 770 and 810 cm⁻¹, respectively. Before distillation, oxidation product has only small peak at 810 cm⁻¹, showing the presence of MBS, but the presence of DMS is unclear due to the low concentration (~1.8 M) of the oxidation product. After distillation, distilled product has a peak at 810 cm⁻¹ with the highest intensity, which indicate MBS is a main component. Peaks corresponding to DMS and SO₃ were also observed as minor intensities at 770 and 730 cm⁻¹. At this moment, it is very difficult to conclude the synthetic path of DMS. It could be synthesized during methane oxidation or it could be formed during vacuum distillation via MBS.

Overall, by a simple vacuum distillation, 84.9% of methane oxidation products, MBS and DMS, could be isolated from the methane oxidation mixture containing sulfuric acid, SO₃ and SO₂. MBS was a major component in the distilled solution. To increase the purity and yield, more sophisticated vacuum distillation or membrane separation technology might be required [32].

4. Conclusions

Pt black catalyzed methane oxidation was conducted under a various reaction conditions. The formation of MBS and CO₂ were heavily affected by the catalyst concentration. The highest MBS yield of 82.1% with a selectivity of 96.5% could be achieved at a

catalyst concentration of 1.6 mM. CO₂, an over-oxidation product, was formed in a substantial amounts when the catalyst concentration was over 30 mM. Based on the approximate estimation of dissolved Pt concentration at the reaction condition, 0.85–1.6 mM, over-oxidation was assumed to happen on the surface of the heterogeneous Pt black. Carbon deposition was also observed on the surface of the Pt black after the reaction, which deteriorated the dissolution of Pt when it was reused. While, Pt ions dissolved in oleum media seemed to retain its catalytic activity through 4 times reaction. Vacuum distillation of the oxidation product was conducted at 130–145 °C under 0.1 mbar and confirmed that MBS could be isolated as a major component.

Acknowledgements

This work was supported by C1 Gas Refinery Program through the National Research Foundation of Korea (NRF) (NRF-2015M3D3A1A01065435).

Appendix A. Supplementary material

Supplementary data to this article can be found online at <https://doi.org/10.1016/j.jcat.2019.04.042>.

References

- [1] N.J. Gunsalus, A. Koppaka, S.H. Park, S.M. Bischof, B.G. Hashiguchi, R.A. Periana, *Chem. Rev.* 117 (2017) 8521.
- [2] M. Ravi, M. Ranocchiaro, J.A. van Bokhoven, *Angew. Chem. Int. Ed.* 56 (2017) 16464.
- [3] S.S. Stahl, J.A. Labinger, J.E. Bercaw, *Angew. Chem. Int. Ed.* 37 (1998) 2180.
- [4] J.H. Lunsford, *Catal. Today* 63 (2000) 165.
- [5] T. Ikuno, J. Zheng, A. Vjunov, M. Sanchez-Sanchez, M.A. Ortuño, D.R. Pahlis, J.L. Fulton, D.M. Camaioni, Z. Li, D. Ray, B.L. Mehdi, N.D. Browning, O.K. Farha, J.T. Hupp, C.J. Cramer, L. Agliardi, J.A. Lercher, *J. Am. Chem. Soc.* 139 (2017) 10294.
- [6] Z. Guo, B. Liu, Q. Zhang, W. Deng, Y. Wang, Y. Yang, *Chem. Soc. Rev.* 43 (2014) 3480.
- [7] M.C. Alvarez-Galvan, N. Mota, M. Ojeda, S. Rojas, R.M. Navarro, J.L.G. Fierro, *Catal. Today* 171 (2011) 15.
- [8] S.E. Bozbag, P. Sot, M. Nachtegaal, M. Ranocchiaro, J.A. van Bokhoven, C. Mesters, *ACS Catal.* 8 (2018) 5721.
- [9] R.A. Periana, D.J. Taube, E.R. Evitt, D.G. Löffler, P.R. Wentrcek, G. Voss, T. Masuda, *Science* 259 (1993) 340.
- [10] R.A. Periana, D.J. Taube, S. Gamble, H. Taube, T. Satoh, H. Fujii, *Science* 280 (1998) 560.
- [11] T. Zimmermann, M. Soorholtz, M. Bilke, F. Schüth, *J. Am. Chem. Soc.* 138 (2016) 12395.
- [12] C.G. Fortman, N.C. Boaz, D. Munz, M.M. Konnick, R.A. Periana, J.T. Groves, T.B. Gunnoe, *J. Am. Chem. Soc.* 136 (2014) 8393.
- [13] J.L. Yuan, L. Liu, L.L. Wang, C.J. Hao, *Catal. Lett.* 143 (2013) 126.
- [14] T. Strassner, S. Ahrens, M. Muehlhofer, D. Munz, A. Zeller, *Eur. J. Inorg. Chem.* 21 (2013) 3659.
- [15] K.J.H. Young, J. Oxgaard, D.H. Ess, S.K. Meier, T. Stewart, W.A. Goddard III, R.A. Periana, *Chem. Commun.* 22 (2009) 3270.
- [16] Z. An, X. Pan, X. Liu, X. Han, X. Bao, *J. Am. Chem. Soc.* 128 (2006) 16028.
- [17] G. Ingrosso, N. Midollini, *J. Mol. Catal. A Chem.* 204 (2003) 425.
- [18] M. Muehlhofer, T. Strassner, W.A. Herrmann, *Angew. Chem. Int. Ed.* 41 (2002) 1745.
- [19] R.A. Periana, O. Mirinov, D.J. Taube, S. Gamble, *Chem. Commun.* 20 (2002) 2376.
- [20] B. Michalkiewicz, *Appl. Catal. A Gen.* 394 (2011) 266.
- [21] X. Gang, Y. Zhu, H. Birch, H.A. Hjuler, N.J. Bjerrum, *Appl. Catal. A Gen.* 261 (2004) 91.
- [22] B. Michalkiewicz, M. Jarosińska, I. Łukasiewicz, *Chem. Eng. J.* 154 (2009) 156.
- [23] T. Zimmermann, M. Bilke, M. Soorholtz, F. Schüth, *ACS Catal.* 8 (2018) 9262.
- [24] H.T. Dang, H.W. Lee, J. Lee, H. Choo, S.H. Hong, M. Cheong, H. Lee, *ACS Catal.* 8 (2018) 11854.
- [25] J. Cheng, Z. Li, M. Haught, Y. Tang, *Chem. Commun.* 44 (2006) 4617.
- [26] R. Palkovits, M. Antonietti, P. Kuhn, A. Thomas, F. Schuth, *Angew. Chem. Int. Ed.* 48 (2009) 6909.
- [27] R. Palkovits, C. von Malotki, M. Baumgarten, K. Mullen, C. Baltes, M. Antonietti, P. Kuhn, J. Weber, A. Thomas, F. Schuth, *ChemSuschem* 3 (2010) 277.
- [28] G. Xiao, CN 001400198A (2003) (to Xiao Gang).
- [29] G. Xiao, X. Hou, B. Li, F. Li, B. Wang, CN 101434514A (2009), to Hanneng Technology Co., Ltd.
- [30] G. Xiao, X. Hou, F. Li, B. Li, B. Wang, CN 101633604A (2013) to Hanergy Tech Co., Ltd.
- [31] R.J. Gillespie, E.A. Robinson, *Can. J. Chem.* 40 (1962) 658.
- [32] B. Michalkiewicz, J. Ziebro, M. Tomaszewska, *J. Mem. Sci.* 286 (2006) 223.